Research on Mesoscale Modeling and Simulation of Selective Laser Melting Process of Quartz Powder

Yating Qiu[1], **Tian Yang**[1], **Wei Han**[1,#]
1 Department of Optical Science and Engineering, Fudan University, 2005 Songhu Road, Yangpu District, Shanghai, China
Corresponding Author / Email: hanw@fudan.edu.cn

KEYWORDS: FLUENT, numerical simulation, laser additive manufacturing, 3D printing, selective laser melting, quartz.

This research focuses on the impact of material spatters, pores, cracks, and other defects on the quality of the quartz samples obtained by selective laser melting, the analyses of the mechanism of defect formation, and how to effectively suppress the defects generation. ANSYS FLUENT software is used to model and simulate the fluid dynamics during the selective laser melting process of quartz powder and deeply simulates and analyzes the formation of the pores and the spattering phenomenon of melt droplets during the melting process. The mechanism of internal defect formation in additive quartz samples is explored by comparing with the simulation results of metal material titanium alloy and researching the influence of quartz material's own characteristics on the thermodynamic dynamics of the melt pool. The results show that the VOF model established in this study can be used to characterize the pores and the spattering phenomenon of melt droplets caused by factors such as evaporation recoil and surface tension during the laser melting process of quartz materials. And through further comparative research, it was found that due to the particularity of quartz materials, the spattering rate is lower than that of metal materials, while the porosity is higher.

1. Introduction

Additive manufacturing technology has developed rapidly in recent years, and its application fields have expanded widely, including aerospace, construction, automobile, etc. Selective laser melting technology is one of the most promising technologies and it could be used on quartz material to process glass crafts and high precision optical parts [1]. Selective laser melting technology is characterized by high laser power, fast scanning speed, and short contact time between laser and powder. However, the present experimental conditions are difficult to quantitatively study the ultra-short time and micro processes. Therefore, it is difficult to characterize the dynamic behavior of the melt pool and the formation process of defects in actual experiments. Besides, the experiment is costly and time-consuming. So the simulation of the selective laser melting can effectively make up the limitations of the experiment, further analyze the reasons and processes for the formation of melt channels and spattering, and explore the mechanism of internal defect formation in the selective laser melting.

At present, many researchers focus on the simulation methods of the laser selective melting. Khairallah et al. [2,3] proposed three important continuous models: melt dynamics without surface tension, adding temperature dependent surface tension to the model and calculation of steam recoil pressure. They also revealed how strong dynamic melt flow generates pore defects, material spattering, and erosion areas through a three-dimensional high-fidelity powder scale model. The influence of recoil pressure and Marangoni convection on melt pool flow, as well as denudation, spatter and pore defects has been studied. Jakumeit et al. [4] simulated the melting and solidification process of metal powder by using Control volume Discretization based on powder bed and substrate and the Eulerian phase method for separating the volume of liquid and gas, and analyzed the influence of process parameters such as laser power and scanning speed on the maximum acceleration of particles in the melt pool. Lang Ming [5] conducted numerical simulation and experimental research on the laser coaxial powder feeding of quartz glass and found that laser power and scanning speed are the two core process parameters of additive manufacturing, which play a significant role in the quality of formed parts. Qu Ruizhi et al. [6] established a high-fidelity powder scale laser melting model for selective laser melting technology, showing the process of powder layer melting, the forming of melt channel and the process of cooling and solidification. By using numerical simulation methods, the evolution process of the spattering phenomenon was reduced, and further research was conducted on the mechanism of melt droplet spattering. It was found that the metal vapor and inert gas flow jointly drive the melt pool flow and droplet spattering behaviors.

Selective laser melting technology uses a laser beam to selectively melt powder materials, forming a high-density formation layer after the solidification of melt liquid. So theoretically, it can be used for various materials [7]. However, quartz has low thermal conductivity and high internal stress. And the high-power laser causes many surface defects such as spatters, keyholes, and cracks during melting and solidification. So it is difficult to achieve complete density in additive manufacturing.

Compared to materials such as metals, plastics, and ceramics, the selective laser melting of quartz is more difficult. Therefore, how to suppress the generation of defects in the selective laser melting of quartz is significantly important. This research aims to establish a suitable VOF model, characterize the selective laser melting process of quartz by using simulation methods, and study the thermodynamic dynamic behavior of the melt pool. And through simulation comparison with the titanium alloy, the effect of quartz material characteristics on the thermodynamic dynamics of the melt pool was studied, and the mechanism of internal defect formation in the additive quartz sample is further explored.

2. Simulation model establishment and result analysis

2.1 Modeling

This research is mainly about the calculation of fluid dynamics. A series of discrete points are used to replace the continuous physical quantities in space. The relationship between the variables on these discrete points is established through the basic conservation equations, and the Algebraic equation is obtained. The approximate values of the actual variables are obtained by calculating and solving the equations, and then the size and distribution of the fundamental physical quantities at each position in the complex flow field are obtained. ANSYS FLUENT was used to simulate the fluid dynamics in the selective laser melting process. The established simulation model is shown in Figure 1. This research focuses on the morphology of the melt pool, melt flow, and droplet spattering in the solid-phase, liquid-phase and gas-phase, considering multiple physical processes, including mass, energy, momentum conservation, latent heat of evaporation, steam recoil and surface tension, and establishing a Gaussian heat source and a discrete model of the powder. The behavior of solid and liquid phases in the melting process was studied by the volume of fluid method. The results analyzed the process of melting and solidification of the melt pool and the formation process of sample defects caused by high temperature evaporation, recoil pressure, Marangoni convection and other factors.

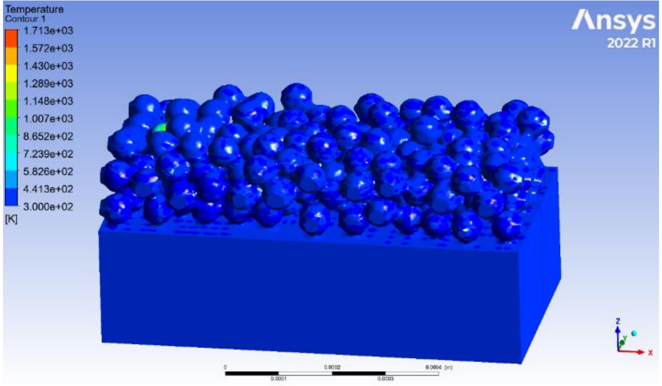

Figure 1 The established model

2.1.1 Heat source

This research uses a laser as an energy source to melt the powder. Due to the loose arrangement of particles in the powder bed, the laser radiates to the surface of the particles and penetrates deep into the powder bed through multiple reflections in the particle gaps. At the same time, most of the energy is reflected and lost. Therefore, in the process of numerical simulation of SLM, the body heat source model with Gaussian distribution is usually chosen. Within the range of the Gaussian body heat source, the volume fraction of solid-liquid phase is obtained through program judgment. If the grid at this location is gas phase, the laser absorption rate A is zero. If the grid is a solid or liquid phase, the laser absorption rate A is non-zero. In the gas-solid and gas-liquid boundary regions, the absorption rate is determined based on the proportion of the volume fraction of each phase in the grid. The expression of the Gaussian volume heat source model is

$$q = \frac{2np}{\pi R^2 s} * \exp\left(-2\frac{r^2}{R^2}\right) * \exp\left(-\frac{z}{s}\right)$$

where, q is the Gaussian heat source, n is the laser absorption rate, p is the laser power, s is the laser penetration depth, r is the distance from the projection point to the initial coordinate when the laser heat source moves, and R is the effective radius of the laser heat source projected onto the powder layer.

2.1.2 Conservation equation

(1) Mass conservation equation

$$\nabla \cdot v = 0$$

(2) Momentum conservation equation

$$\frac{\partial v}{\partial t} + (v \cdot \nabla)v = -\frac{1}{\rho}\nabla p + \mu\nabla^2 v + g[1 - \beta(T - T_m)]$$

(3) Energy conservation equation

$$\frac{\partial h}{\partial t} + (v \cdot \nabla)h = \frac{1}{\rho}(\nabla \cdot \mathrm{k}\nabla \mathrm{T})$$

In these formulas, v is the melt flow rate, μ is the viscosity, β is the coefficient of thermal expansion, h is the enthalpy value, k is the thermal conductivity, T_m is the liquidus.

2.1.3 Boundary conditions

The boundary conditions of this simulation are the heat exchange between the outer surfaces of each phase and the surrounding environment, mainly including Newtonian convective heat transfer and thermal radiation.

When heat exchange occurs between the material at the boundary and the surrounding medium,

$$-k\nabla T = h(T - T_a)$$

h is the heat transfer coefficient and T_a is the ambient temperature.

When thermal radiation occurs at the boundary,

$$-k\nabla T = \sigma\varepsilon(T^4 - T_a^4)$$

σ is the Stefen Boltzmann constant and ε is the thermal radiation coefficient.

2.1.4 Condition settings

The expression for evaporation loss is

$$q_v = -0.82\frac{\mathrm{Lv} * \mathrm{M}}{\sqrt{2\pi MRT}} P_0 \exp\left(\frac{\mathrm{Lv} * \mathrm{M} * (\mathrm{T} - \mathrm{Tv})}{\mathrm{R} * \mathrm{T} * \mathrm{Tv}}\right)$$

The expression for steam recoil force is

$$F_{\text{recoil}} = 0.54P_0 * \exp\,(\mathrm{Lv} * \mathrm{M} * (\mathrm{T} - \mathrm{Tv})\,/\,(\mathrm{R} * \mathrm{T} * \mathrm{Tv}))$$

where, q_v is the evaporation loss, F_{recoil} is the steam recoil force, P_0 is the saturated vapor pressure, Lv is the latent heat of evaporation, M is the molar mass, Tv is the evaporation temperature, and R is the constant of the ideal gas.

The expression for surface tension is

$$\gamma = 0.278 - 0.00027(T - T_1)$$

where, γ is the surface tension, and T_1 is the liquidus. [8]

2.1.5 Assumptions

For the convenience of model calculation, the following assumptions are set.

(1) Neglecting the heat loss caused by the decomposition of silica;

(2) Powder size and shape are the same;

(3) The fluid flow is laminar and incompressible;

(4) The thermal convection coefficient is a constant value;

(5) Ignore light pressure;

(6) Neglecting heat transfer caused by convection, thermal radiation, and thermal expansion.

2.2 Simulation results

Firstly, a simulation model was established for the selective laser melting of quartz powder to analyze the melting and solidification process. The simulation results are shown in Figure 2 to Figure 4.

According to Figure 2, (a) At 1ms, the laser heat source irradiates onto the powder, and the particles begin to melt, resulting in a melting zone; (b) At 4ms, the laser moves in the x direction, the front part of the melt pool directly absorbs the laser energy, and the tail of the melt pool is not completely cooled; (c) At 7ms, the tail of the melt pool is partially cooled, and a fracture occurs between the front section of the melt pool and the tail of the melt pool, resulting in surface defects; (d) At 10ms, the laser heat source continued to move in the x direction, and the tail of the melt pool gradually cooled; (e) At 20ms, the monorail scanning ends, the scanning area of the first rail shows incomplete melting and surface defects caused by fusing. The laser heat source begins the second rail scanning, and the light source moves 0.055mm along the -y axis, also moving in the positive direction of the x axis; (f) At 25ms, the parts of the melt pool that have been cooled are scanned for remelting, and the melt pool is relatively widened and lengthened because the first rail not thoroughly cooled down; (g) At 30ms, the broken part of the monorail printing was remelted, and the melting effect was significantly better than that of the monorail scan; (h) At 40ms, the double track scan ended, and there were still obvious surface defects, but the melting effect was better than that of the monorail scan.

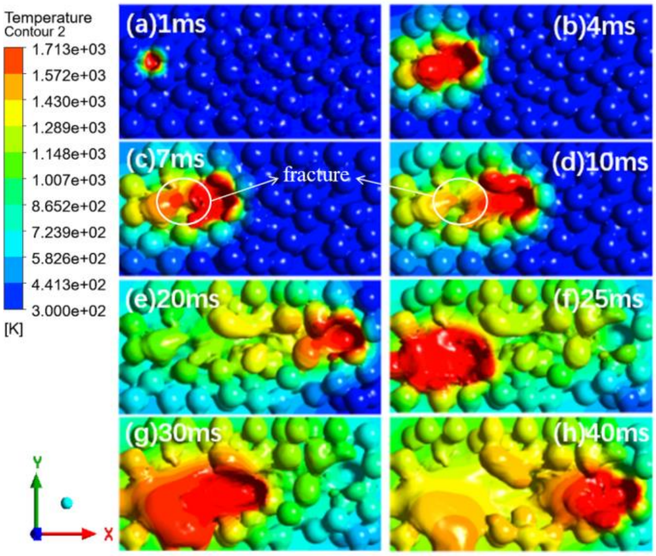

Figure 2 Simulation results of the selective laser melting of quartz powder

Figure 3 shows the formation of pores in the quartz melt pool. The melt pool is heated by a laser and forms a concave keyhole. The main driving forces for the instability of melt flow were considered as the Marangoni and recoil forces [9]. The flowing liquid above the pore bottom flows and merges towards the center due to the Marangoni convection, resulting in the formation of pore bubbles in areas that have not been fused in time. The bubbles flow with the melt pool driven by Marangoni effect, and the bubbles that are not transported out in time stay in the melt pool and form pore defects of the quartz molding parts after solidification.

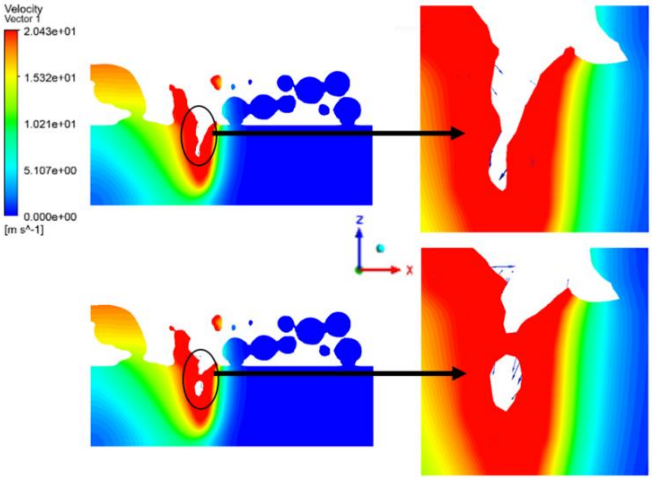

Figure 3 Keyhole flow velocity vector

Figure 4 shows the spatter formation in the quartz melt pool. In the simulation process, there are droplets spattering out of the melt pool and falling back into the melt pool or falling into the unmelted area. The droplet spatters are generated from the unstable melt pool under the action of steam recoil force and Marangoni effect due to the unstable boiling state during the melting and solidification process of the melt pool. And they lead to the pollution of the powder bed and the formation of defects in the process of falling back. During the melting of each layer, droplets that fall back onto the powder surface increase surface roughness and porosity.

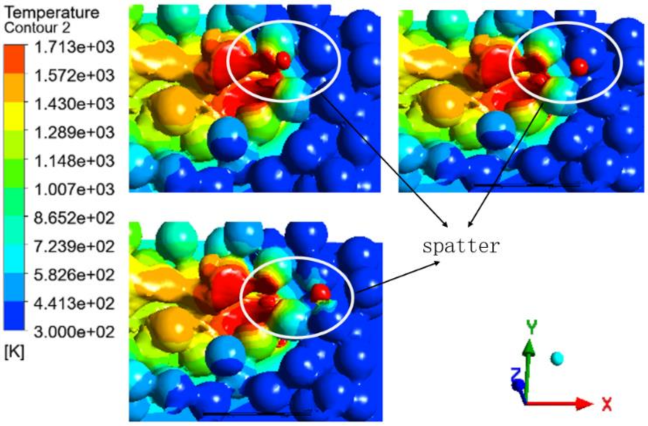

Figure 4 Droplet spattering process

In order to further study the factors affecting the defects formation in the selective laser melting process of quartz powder, the selective laser melting processes of the quartz and metal (titanium alloy) powder were simulated and compared under the same laser power and scanning speed conditions. The results are shown in Figure 5 to Figure 8. It can be clearly seen that there is a significant difference in the melting of quartz and metal materials at the same laser power and scanning speed.

Figure 5 shows the three-dimensional shape of the melt pool. Quartz is prone to fracture during the melting process, and there is a continuous melt pool orbit during the metal melting process. Figure 6 shows the side profile of the keyhole morphology , and the keyhole depth of the quartz material is obviously larger than that of the metal material. Figure 7 shows the flow velocity vector of the melt pool in the top view, and Figure 8 shows the flow velocity vector of the melt pool in the side profile. It is different in the size and direction of the flow velocity vector of the melt pool of different materials near the direct laser irradiation area. The formation mechanism of a quartz glass melt pool is driven by melt pool wetting and viscous flow. The low-viscosity melt (metal) tends to form droplet spatters, which are caused by strong Marangoni flow and recoil force. The high-viscosity material (quartz) prevents spatter formation by reducing the Marangoni flow. The flow of the melt pool driven by Marangoni effect also facilitates pore transport and gas release. During the melting of the metal, Marangoni force makes it easier to transport the bubbles out of the melt pool. While in the melt pool of quartz glass, the viscous flow behavior limits the transport of pores, and it is easier to retain pore bubbles. And due to the boiling behavior of the melt pool, the pores are promoted to merge and expand, so the porosity is higher [10].

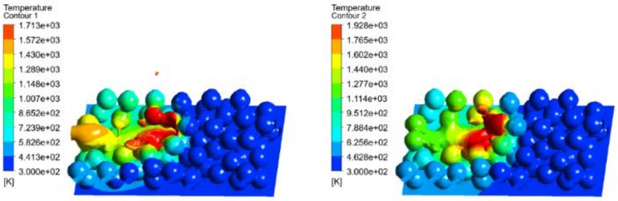

(a) Quartz (b) Titanium alloy

Figure 5 Three-dimensional shape of the melt pool

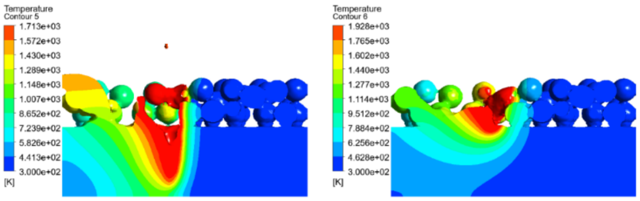

(a) Quartz (b) Titanium alloy

Figure 6 Keyhole morphology of the side profile

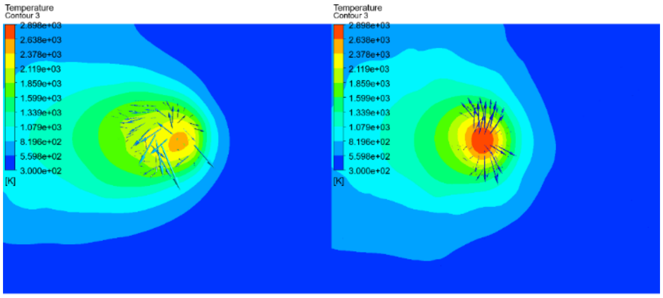

(a) Quartz (b) Titanium alloy

Figure 7 Flow velocity vector of the melt pool in the top view

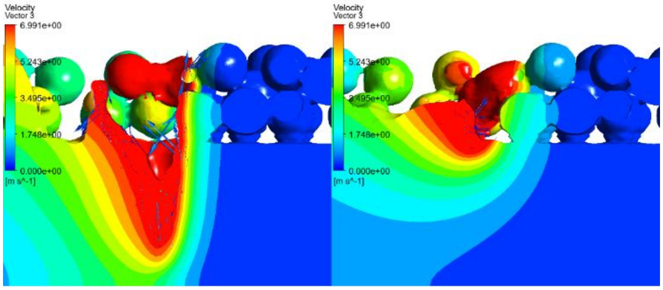

(a) Quartz (b) Titanium alloy

Figure 8 Flow velocity vector of the melt pool in the side profile

3. Conclusions

In this paper, a numerical simulation model of selective laser melting is proposed to describe the melting and solidification of quartz powder. The model can reproduce the flow form of melt pool formed by the quartz powder irradiated by the laser beam, simulate the actual process of melting and collapsing deformation of particles and the specific morphology of the surface roughness of melt pool. The numerical simulation results show that the defects such as spatter and porosity are unavoidable during the selective laser melting of quartz materials. And because of the influence of quartz material's physical characteristics, compared with metal materials, it has less spatters and more pores. In the process of actual simulation operation, the most difficult technical difficulties are the mutual conversion between solid phase and liquid phase and the calculation of steam recoil pressure. The simulation model can also be further optimized to obtain more realistic simulation results, simulating more realistic spattering effects and internal pores of the sample.

REFERENCES

1. Dao ZHANG, Xiaofeng LIU, Jianrong QIU. 3D printing of glass by additive manufacturing techniques: a review. Front. Optoelectron., 2021, 14(3): 263–277.
2. Khairallah, S.A., A. Anderson, A.M. Rubenchik, J. Florando, S. Wu, and H. Lowdermilk. "Simulation of the Main Physical Processes in Remote Laser Penetration with Large Laser Spot Size." AIP Advances 5.4 (2015): 47120-047120-10.
3. Khairallah, Saad A., Andrew T. Anderson, Alexander Rubenchik, and Wayne E. King. "Laser Powder-bed Fusion Additive Manufacturing: Physics of Complex Melt Flow and Formation Mechanisms of Pores, Spatter, and Denudation Zones." Acta Materialia 108.C (2016): 36-45.
4. Jakumeit, Jürgen, Gongyuan Zheng, Romuald Laqua, Samuel J. Clark, Jonas Zielinski, Johannes H. Schleifenbaum, and Peter D. Lee. "Modelling the Complex Evaporated Gas Flow and Its Impact on Particle Spattering during Laser Powder Bed Fusion." Additive Manufacturing 47 (2021): 102332.
5. Lang Ming. Numerical simulation and experimental research on the manufacture of quartz glass by laser coaxial powder feeding additive [D]. University of the Chinese Academy of Sciences (Institute of Optics and Electronics), 2022.
6. Qu, Ruizhi, Liangpei Huang, and Dongming Xiao. " Numerical simulation of melt pool evolution and metal splashing characteristics during selective laser melting process" Hang Kong Xue Bao 43.4 (2022): 398-417.
7. R.S. Khmyrov, S.N. Grigoriev, A.A. Okunkova, A.V. Gusarov. On the Possibility of Selective Laser Melting of Quartz Glass.[J] Physics Procedia, 56 (2014) 345–356.
8. N.M. Parikh, Effect of atmosphere on surface tension of glass, J. Am. Ceram. Soc. 41, 18–22 (1958).
9. Qiu, Chunlei, Chinnapat Panwisawas, Mark Ward, Hector C. Basoalto, Jeffery W. Brooks, and Moataz M. Attallah. "On the Role of Melt Flow into the Surface Structure and Porosity Development during Selective Laser Melting." Acta Materialia 96 (2015): 72-79. Web.
10. LEUNG C L A, MARUSSI S, TOWRIE M, et al. The effect of powder oxidation on defect formation in laser additive manufacturing[J/OL]. Acta Materialia, 2019, 166: 294-305.